ADANA ALPARSLAN TÜRKEŞ BİLİM VE TEKNOLOJİ ÜNİVERSİTESİ BİLİM DERGİSİ

ADANA ALPARSLAN TÜRKEŞ SCIENCE AND TECHNOLOGY UNIVERSITY JOURNAL OF SCIENCE

Research Article www.dergipark.com/atujscience

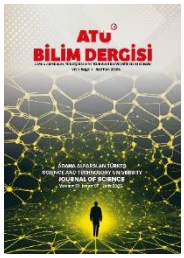

Bio-Heat Transfer in Cancer Treatment: A Mathematical Framework for Hyperthermia-Assisted Radiotherapy Using Monte Carlo Simulation

Tuka Fattal[1#], Birnur Bozdoğan[2], Recep Yumrutaş[3]

(This study was presented at ULIBTK'25 congress)

Abstract

This study explores bio-heat transfer during radiotherapy combined with hyperthermia, with the goal of improving cancer treatment by maximizing tumor destruction while minimizing harm to surrounding healthy tissue. Understanding thermal dynamics during therapy allows clinicians to enhance treatment effectiveness, anticipate biological responses based on dose parameters, and reduce side effects. In this work, we focus on the synergistic use of hyperthermia and X-ray radiotherapy. During short recovery periods between hyperthermia pulses—when tissue responds to elevated temperatures (43 °C, 45 °C, 47 °C)—radiation is delivered. The central hypothesis is that heating tumor tissue increases its radiosensitivity, potentially shortening treatment time and improving outcomes. Evidence from current literature supports this synergy, showing that higher temperatures amplify cellular damage. To quantify this effect, we applied the Arrhenius damage model, which converts temperature and exposure duration into a single thermal damage parameter (Ω) representing irreversible tissue injury. Finally, we developed a mathematical framework to simulate this process, using Monte Carlo photon transport to generate spatial heat sources and solving Pennes' bio-heat equation to model heat transfer across layered biological tissue.

Keywords: Heat transfer; Pennes' bioheat equation; cancer treatment; radiotherapy; X-ray hyperthermia; Monti Carlo simulation.

[1,2,3]Gaziantep University, Faculty of Engineering, Mechanical Engineering Department, 27310 Şehitkamil, Gaziantep, Türkiye

ORCID[1]: 0009-0007-5413-6148

ORCID[2]: 0000-0003-0314-837X

ORCID[3]: 0000-0001-9006-198X

#Corresponding Author:
drtukafattal78@gmail.com

Kanser Tedavisinde Biyo-Isı Transferi: Monte Carlo Simülasyonu Kullanılarak Hipertermi Destekli Radyoterapi İçin Matematiksel Bir Çerçeve

(Bu çalışma ULIBTK'25 kongresinde sunulmuştur)

Öz

Bu çalışma, kanser hücrelerine yönelik radyasyon tedavisi (radyoterapi) sırasında hipertermi yoluyla gerçekleşen biyoısı transferini özel olarak incelemeyi amaçlamaktadır. Bu inceleme, tedavi sonuçlarını optimize etmek, kanser hücrelerini yok etmek ve sağlıklı dokular üzerindeki yan etkileri (toksisiteyi) önlemek açısından önem taşımaktadır. Tedavi sırasında gerçekleşen ısı transferi sürecinin anlaşılması, hekimlerin tedavi etkilerini maksimize etmesine, uygulanan dozlara bağlı tepkileri öngörmesine ve yan etkileri en aza indirmesine yardımcı olabilir. X-ışını kullanan radyoterapi ile hiperterminin kombinasyonu, kanser hücrelerinin tedavisinde kullanılan yöntemler arasında özel olarak araştırılmıştır. Bu araştırma, her iki yöntemin avantajlarını bir araya getirmeyi ve bunlarla ilişkili istenmeyen yan etkileri azaltmayı hedeflemektedir. İki hipertermi darbesi arasındaki dinlenme süresi boyunca, biyolojik sistem uygulanan yüksek sıcaklıklara (43°C, 45°C, 47°C) karşı tepki vermeye çalışırken, radyoterapi dozu uygulanmaktadır. Ana fikir şudur: Kanser hücrelerinin ısıtılması, onları radyasyon tedavisine karşı daha hassas hale getirir; bu da tedavi süresini kısaltabilir, yan etkileri azaltabilir ve hayatta kalma oranlarını artırabilir. Yapılan literatür taramasına göre, kanser hücrelerinin artışı daha fazla doku hasarına yol açmaktadır. Bu bağlamda, Arrhenius modeli kullanılarak sıcaklık ve ısıya maruz kalma süresinin artmasının, kanser hücrelerine verilen hasarı artırdığı gösterilmiştir. Bu model, sıcaklık ve maruziyet süresi parametrelerini, geri dönüşü olmayan doku hasarını yansıtan tek bir parametreye (Ω) dönüştürmektedir. Son olarak, Pennes'in biyoısı denklemini çözmek için Monte Carlo Simülasyonu kullanılarak radyoterapi tedavisine yönelik genel bir biyoısı transferi matematiksel çerçevesi sunulmuştur.

Anahtar Kelimeler: Isı transferi; Pennes'in biyoısı denklemi; kanser tedavisi; radyoterapi; X-ışını hipertermisi; Monte Carlo simülasyonu.

Received: 27/10/2025

Accepted: 10/12/2025

Online Published: 25/12/2025

How to Cite: Fattal T., Bozdoğan B., Yumrutaş R. "*Bio-Heat Transfer in Cancer Treatment: A Mathematical Framework for Hyperthermia-Assisted Radiotherapy Using Monte Carlo Simulation*" Adana Alparslan Türkeş Science and Technology University Journal of Science, **1** (2): 96-109 (2025).

1. Introduction

Radiation therapy is one of the most common cancer treatments. Its clinical use began in the early 20th century following the discoveries of X-rays by Roentgen (1895) and the Curie's work on radium in 1898. Radiotherapy can be delivered alone or combined with chemotherapy or surgery to improve cure rates. Precise dosing is critical: it must destroy the tumor while sparing nearby healthy tissues, which is the primary clinical challenge of radiotherapy. Including radiotherapy infrastructure in national cancer plans ensures both early detection and broad access to effective treatment. Careful prediction of the coagulation zone—the area of irreversible tissue damage—is essential to avoid unintended harm and allow normal, tissue recovery [1]. A well-designed treatment plan must balance full tumor ablation with minimizing toxicity to adjacent organs, nerves, and blood vessel. Hyperthermia as a cancer treatment dates back to ancient times but gained modern attention in the 19th century when William B. Coley induced fevers to shrink tumors. Typically, cancer cells are exposed to temperatures around 44–45 °C for about an hour. Elevated temperature disrupts cancer cell proteins, DNA repair, and tumor blood flow—affecting the tumor microenvironment, immunity, and vascularization—with minimal impact on normal tissues [2] [3] Combining radiotherapy and hyperthermia ("thermoradiotherapy") has been used since the 1970s and shows improved outcomes in advanced cancers (e.g., breast, cervical, head-and-neck, bladder, soft tissue sarcoma, melanoma) without increased serious side effects. Clinical trials confirm significantly higher complete response rates with thermoradiotherapy versus radiotherapy alone, and logistical studies show close timing between heat and radiation enhances efficacy while sparing healthy tissue [4] [5].

2. Literature Review

Recent research into the physiological mechanisms behind thermoradiotherapy (TRT) has made its synergy increasingly promising. However, several questions remain unresolved:

- What is the optimal hyperthermia temperature and duration to achieve maximal radiosensitization without triggering thermotolerance?
- How does hyperthermia impact DNA repair pathways in tumor versus healthy cells?[6]

Precision radiotherapy combined with nanoparticle-mediated hyperthermia shows great potential. Injected nanoparticles—such as gold, gadolinium, or magnetic particles—accumulate in tumors, enabling highly focused heating that intensifies DNA damage and boosts radiotherapy effectiveness [7]**.** Beyond TRT, hyperthermia plus chemotherapy has demonstrated improved long-term outcomes. For example, a JAMA Oncology trial (EORTC 62961–ESHO-95) reported an 11.4% gain in 5-year survival when regional hyperthermia was added to neoadjuvant chemotherapy for soft tissue sarcoma. The principle is simple but powerful: heat enhances blood flow and oxygenation, improving drug uptake in tumors without damaging healthy surrounding tissue [8] [9]. In Turkey, several clinical studies illustrate TRT's real-world impact:

- 2017, Yıldırım Beyazıt University (Ankara): Locoregional recurrent breast cancer treated with radiotherapy + hyperthermia achieved higher local control and low toxicity [10].
- 2023, Istanbul (ASCO abstract): Combining chemotherapy with radiofrequency hyperthermia (Oncothermia, 45 °C) in metastatic colorectal cancer produced a 96% objective response rate, with no unexpected toxicity [11]

Across Turkey, hyperthermia use—particularly in locally advanced or recurrent cancers (breast, cervical, lung, colorectal, rectal)—has grown steadily. Several major oncology centers now integrate it alongside radiotherapy, although literature is still heavily based on smaller trials and case reports [12]. Despite encouraging early results, TRT+HT remains understudied. Most available evidence stems from small-scale phase II trials or single-center studies. There is a pressing need for larger, well-controlled clinical trials to:

1. Pinpoint optimal HT dose, duration, and timing in relation to RT.
2. Validate nanoparticle and Oncothermia enhancements.
3. Expand TRT's adoption into standard cancer care protocols [13].

3. Methodology

In this study, we investigated a hybrid cancer treatment that combines laser-induced hyperthermia with X-ray radiotherapy, aiming to destroy cancer cells while minimizing damage to healthy tissues. To do this, we created a synthetic 3D lung-tumor model using advanced computational techniques and realistic treatment conditions.

- Laser Hyperthermia Application: We used an external laser to increase tumor temperature in distinct phases—43 °C, 45 °C, and 47 °C—mirroring established LITT (Laser-Induced Thermal Treatment) protocols [14].
- Monte Carlo Heat Deposition (MCXLAB): For each temperature stage, we mapped 3D energy deposition using MCXLAB, a GPU-accelerated Monte Carlo photon transport toolkit. The result was a detailed spatial heat-source term integrated into Pennes' bio-heat equation to simulate temperature evolution over time [15] [16]. Monte Carlo (MC) methods are a class of computational algorithms that rely on statistical

sampling to solve complex physical and mathematical problems. In radiation transport, MC simulates probabilistic interactions of photons as they traverse tissue, including scattering, absorption, and secondary particle generation, based on known cross-sections. This approach provides highly accurate dose distributions in heterogeneous and geometrically complex media, outperforming deterministic models. In this study, MC simulations were used to calculate spatial energy deposition during X-ray radiotherapy. The resulting dose map was converted into a volumetric heat source term for Pennes' bio-heat equation, enabling realistic modeling of thermal dynamics during combined hyperthermia and radiotherapy.

- Arrhenius Thermal Damage Assessment: We employed the Arrhenius model to estimate irreversible thermal damage caused by heating cancer cells [17].
- X-ray Dose & Radiobiological Effect (LQ model). After each hyperthermia pulse, we simulated X-ray dose distribution using Monte Carlo methods and evaluated cell survival using the Linear–Quadratic (LQ) model [18].
- Comparative Evaluation Across Temperatures: We compared thermal damage and radiation effectiveness at 43 °C, 45 °C, and 47 °C to determine which offered optimal tumor destruction with minimal harm to healthy tissue. To efficiently simulate heat transfer, we assumed a spherically symmetric tumor control volume with concentric healthy lung tissue layers.
- Radial Symmetry & Boundary Conditions:
    - Symmetry at the tumor core (r = 0).
    - Convective heat loss at the outer surface.
    - Blood perfusion included throughout the tissue [19]
- Bio-Heat Equation Formulation**:** We used Pennes' bio-heat model in spherical coordinates to predict transient temperature changes during and after heating [16].

Penn's bioheat equation was solved using temperatures in Celsius because it involves temperature differences (e.g., $T_a - T_{(r,T)}$), where adding 273.15 to both terms cancels out, making °C practical for interpretation. However, the Arrhenius thermal damage model requires absolute temperature in Kelvin because its exponential term depends on absolute energy states. To ensure consistency and accuracy, all temperature data used in the damage calculations was converted from Celsius to Kelvin before applying the Arrhenius model.

Figure 1 shows the idealized spherical control volume used to model heat transfer during hyperthermia treatment. At the center lies the tumor, surrounded by concentric layers of healthy lung tissue. This geometry enables the use of spherical coordinates (r, θ, ϕ), which naturally capture radial heat diffusion and laser energy deposition. A symmetry condition at the tumor core (r = 0) ensures no heat flux, while the outer boundary (r = R) applies a convective heat-loss condition to represent thermal exchange with surrounding tissue. Internal heat sources include metabolic activity, blood perfusion, and laser energy derived from Monte Carlo photon transport simulations. This configuration forms the basis for solving the time-dependent Pennes' bio-heat equation, allowing prediction of temperature rise and thermal damage across the tumor and adjacent tissue under controlled heating phases (43 °C, 45 °C, and 47 °C) [20]. We adopted 47 °C as the upper limit to distinguish hyperthermia from thermal ablative therapy. Temperatures above this threshold enter a zone where irreversible tissue damage and collateral thermal injury become significant, aligning with literature that defines hyperthermia as 39–45 °C and ablative therapy as ≥50 °C [21], [22]

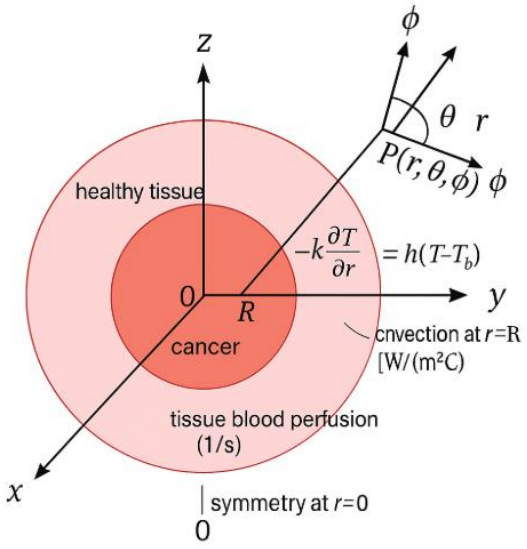

Figure 1. Spherical tumor-embedded control volume for bio-heat transfer analysis.

3.1 Initial Anatomical Model

To simulate heat transfer during hyperthermia, we constructed a radially symmetric anatomical model that represents a solid tumor embedded within healthy tissue. Figure 2, illustrates the voxel-based phantom, which provides an idealized yet practical framework for thermal analysis. Its spherical geometry enables the use of spherical coordinates (r, θ, ϕ), perfectly suited for capturing radial heat diffusion and energy deposition. At the center lies the tumor region, while surrounding layers represent healthy tissue. This symmetry minimizes numerical artifacts and ensures smooth propagation of heat gradients from the core outward. The phantom's modular design also allows easy labeling of tissue layers—such as tumor, fat, muscle, and skin—supporting later stages of multi-layer thermal and radiative modeling [16].

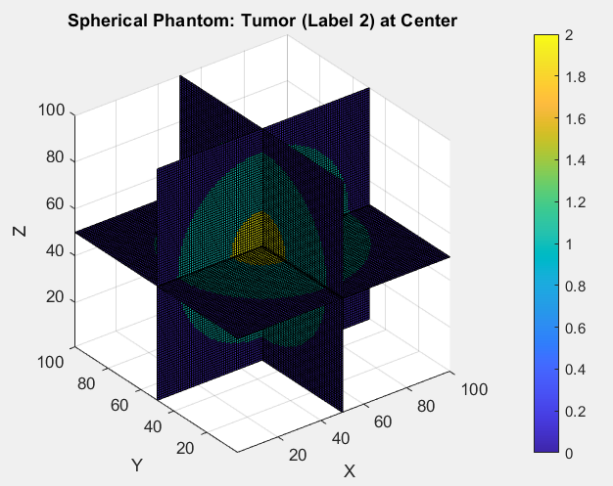

Figure 2. Voxelized 3D spherical phantom with central tumor (Label 2) and surrounding healthy tissue (Label 1).

3.2 Heating Phase 1: Heating Tumor Tissue to 43°C

3.2.1 Heating Tumor Tissue to 43°C

In the first hyperthermia stage, the tumor core was heated to 43 °C using an external laser source. To accurately model light propagation through tissue, we employed MCXLAB, a Monte Carlo-based simulation tool that calculates photon transport within the layered 3D anatomical phantom. The resulting fluence map was converted into a spatially varying heat source term, $Q_{laser}(r)$, which was then integrated into the time-dependent Pennes bio-heat equation expressed in spherical coordinates, as illustrated below [20]:

$$\rho c\,\frac{\partial T(r,t)}{\partial t} = \frac{1}{r^2}\,\frac{\partial}{\partial r}\left(r^2 K\,\frac{T(r,t)}{\partial r}\right) + \rho_b C_b\,\omega_b\big(T_a - T(r,t)\big) + Q_{met} + Q_{laser(r)}$$

This formulation accounts for radial heat conduction, perfusion loss, baseline metabolism $Q_{met}$and laser-induced heating [23]. This method discretizes the equation in both time and space to simulate the transient temperature distribution within tissue subjected to laser heating and perfusion. The finite difference scheme was applied as follows:

- Time derivative (forward difference):

$$\frac{\partial T}{\partial t} \approx \frac{T_i^{n+1} - T_i^n}{\Delta t}$$

- Spatial derivative in spherical form (central difference):

$$\frac{1}{r^2}\frac{\partial}{\partial r}\left(r^2\,\frac{\partial T}{\partial r}\right) \approx \frac{1}{r_i^2}\left[\frac{r_{i+0.5}^2(T_{i+1}^n - T_i^n) - r_{i-0.5}^2(T_i^n - T_{i-1}^n)}{\Delta r^2}\right]$$

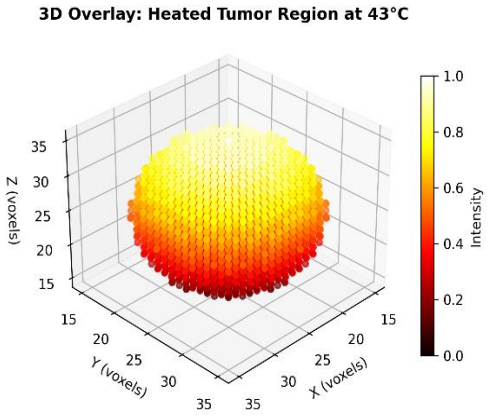

Figure 3. 3D overlay: heated tumor region at 43°C.

The equation was solved numerically over time to simulate the transient temperature response across the control volume. The simulation confirmed that the tumor core successfully reached 43 °C after approximately 900 seconds (15 minutes) of continuous laser exposure. Figure 3 shows a 3D overlay of the heated tumor region, highlighting the region that achieved the target temperature.

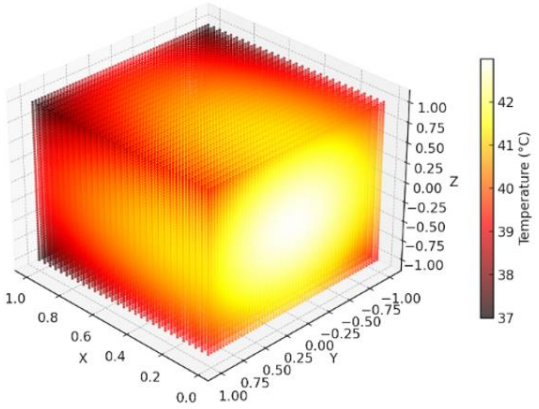

Figure 4. Cutaway view: heat distribution in tumor & surrounding tissues.

Figure 4 presents a 3D cutaway visualization of temperature distribution across the layered tissue model following laser-induced heating. The image highlights how heat radiates outward from the tumor core—the hottest region—through adjacent layers of muscle, fat, and skin. The thermal gradient, ranging from approximately 43 °C at the tumor center to ~37 °C near the outer boundary, reflects realistic heat diffusion governed by Pennes' bio-heat equation. This pattern demonstrates the combined effects of conduction and biological cooling mechanisms such as blood perfusion. The smooth, radially symmetric temperature profile confirms that the heating phase was accurately implemented and maintained within safe limits for surrounding healthy tissue.

3.2.2 Estimating Thermal Damage

To evaluate the biological impact of heating the tumor to 43 °C, the Arrhenius thermal damage model was employed. This model is widely accepted for quantifying irreversible molecular injury caused by temperature elevation in biological tissues. It estimates the damage index, Ω(t), which reflects the logarithmic ratio of healthy to surviving molecules over time, and is sensitive to both temperature and exposure duration. The model uses the following integral expression [24]:

$$\Omega(t) = \int_0^t A.\exp\left(-\frac{E_a}{RT(\tau)}\right) d\tau$$

Where:

- Ω(t): Accumulated thermal damage index (unitless)
- A: Frequency factor (s^{-1}), representing molecular reaction rate
- E_a : Activation energy, specific to tissue type
- R: Universal gas constant.

- $T(\tau)$: Absolute temperature (in Kelvin) as a function of time
- Ω: Dimensionless damage index ($\Omega \geq 1$ means irreversible damage).

Using the temperature-time profiles obtained from solving the Pennes' bio-heat equation, the Arrhenius thermal damage integral was numerically evaluated across the tumor and surrounding tissues. The results, shown in Figure 5, indicate that thermal damage values reached $\Omega \approx 0.005$ in the tumor center, reflecting sub-lethal injury, consistent with the goal of sensitizing cancer cells to subsequent radiotherapy without inducing irreversible ablation. Peripheral layers exhibited even lower damage values, further confirming the spatial selectivity of laser-based hyperthermia.

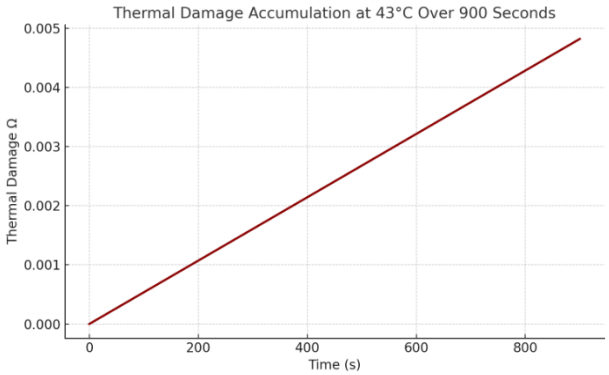

Figure 5. Thermal damage accumulation at 43°C over 900 seconds.

3.2.3 X-ray Application During Relaxation (Post-Heating Phase 1).

After raising the tumor temperature to 43 °C using laser-based hyperthermia, we delivered a targeted radiotherapy dose. A 6 MeV collimated X-ray beam was applied during the 5-minute thermal relaxation period—timed deliberately to take advantage of the radiosensitized state of tumor cells. This approach aims to maximize treatment effectiveness while minimizing exposure to healthy tissue. Photon transport and 3D dose distribution were modeled using Monte Carlo simulations (MCXLAB). As shown in Figure 6, the dose concentrated at the tumor core with a smooth Gaussian falloff, ensuring precise targeting and reduced peripheral impact.

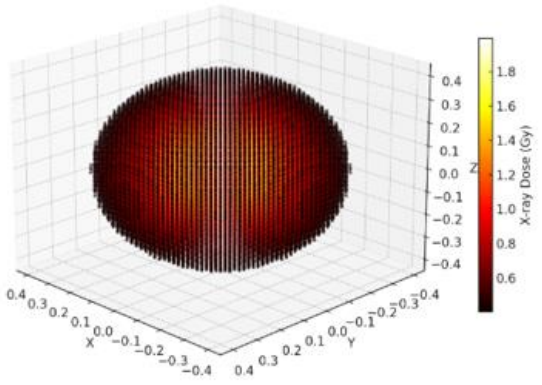

Figure 6. 3D spatial distribution of x-ray dose following laser-ınduced hyperthermia at 43 °C.

3.2.4 Combined Damage Assessment (Thermal + X-ray)

To quantify the combined effect of hyperthermia and radiotherapy, we computed the Effective Damage (ED)—the predicted fraction of cell death under both thermal and radiation stress. This metric integrates the Arrhenius thermal injury model with the Linear-Quadratic (LQ) radiobiological model, capturing their synergistic potential. Figure 7 illustrates the 3D rendering of cell death probability, where each voxel represents irreversible damage likelihood. The tumor core shows the highest ED values (≈0.9), confirming that sequential treatment significantly improves lethality compared to hyperthermia alone. Damage decreases toward the periphery, validating selective tumor targeting while sparing healthy tissue. These results reinforce the study's central

hypothesis: moderate hyperthermia (43 °C) enhances radiosensitivity, enabling better outcomes without increasing radiation dose or exceeding safe thermal limits.

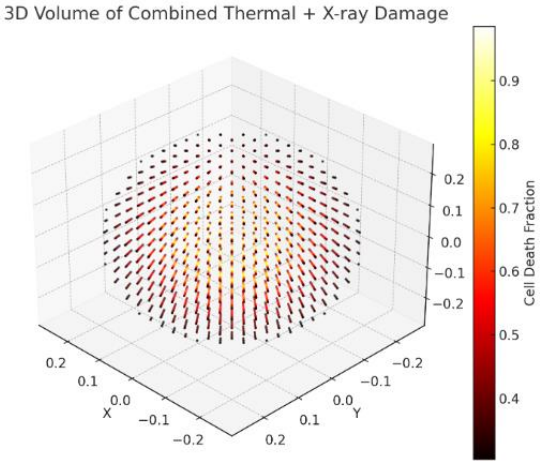

Figure 7. 3D visualization of effective cell death from combined hyperthermia and x-ray treatment.

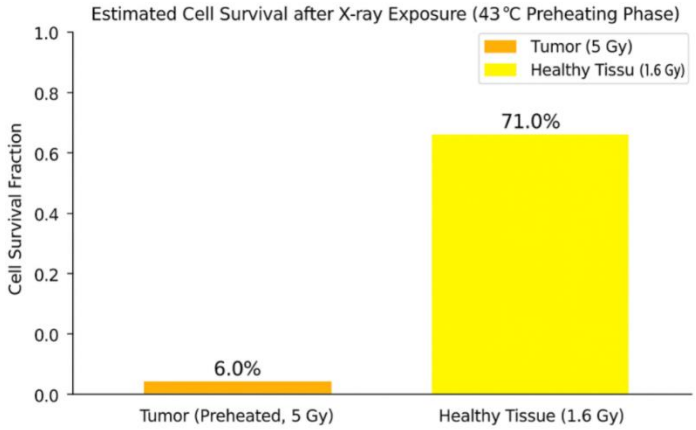

Figure 8. Cell survival comparison following 43 °c hyperthermia and radiotherapy (first treatment phase).

The survival analysis clearly demonstrates the selective effectiveness of the combined treatment. When the tumor was heated to 43 °C and then exposed to a 5 Gy X-ray dose, cell viability dropped dramatically—only about **6**% of tumor cells survived. In contrast, healthy tissue, which received a much lower dose (≈1.6 Gy due to spatial attenuation), retained 71% survival, indicating that normal structures were largely preserved. These findings strongly support the concept that moderate hyperthermia enhances radiosensitivity, improving therapeutic outcomes without increasing radiation dose—a critical advantage in clinical practice where protecting healthy tissue is essential. Figure 8 illustrates the survival comparison between tumor and healthy cells.

3.3 Heating Phase 2: Heating Tumor Tissue to 45°C

3.3.1 Heating Tumor Tissue to 45°C

To assess the effect of a higher thermal dose, the second phase targeted a tumor temperature of 45 °C using the same anatomical model and boundary conditions for consistency. Before initiating this stage, tissue was assumed to have cooled back to its baseline temperature (37 °C), reflecting a realistic recovery period. The simulation followed the established workflow—laser heating, bio-heat modeling, thermal damage estimation, and subsequent radiotherapy—while extending the heating duration to approximately 1,200 seconds to reach the new target. This controlled approach enabled a direct comparison of thermal response and radiosensitization between the two temperature levels. The accompanying visualization illustrates the internal temperature distribution during this phase. Heat is concentrated at the tumor core, achieving the 45 °C target, and gradually decreases toward the outer layers. The cutaway view highlights the smooth thermal gradient across the 3D volume, confirming effective localized hyperthermia (Figure 9).

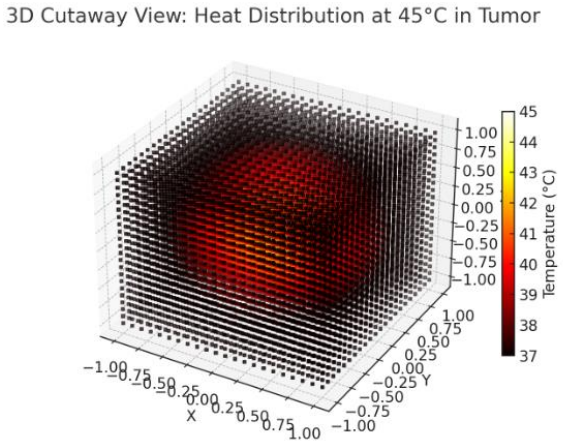

Figure 9. 3D cutaway view: heat distribution in tumor and tissues at 45°C.

3.3.2 Estimating Thermal Damage

During the second heating phase, the tumor was reheated from 37 °C to 45 °C using laser-based hyperthermia. Thermal damage estimation via the Arrhenius mode. At this temperature, the Arrhenius thermal damage index reached approximately Ω ≈ 0.010, which is about twice the damage observed at 43 °C (Ω ≈ 0.005). This indicates a sharper rise in thermal injury, demonstrating the increased effect of hyperthermia with just a 2 °C temperature increase (Figure 10).

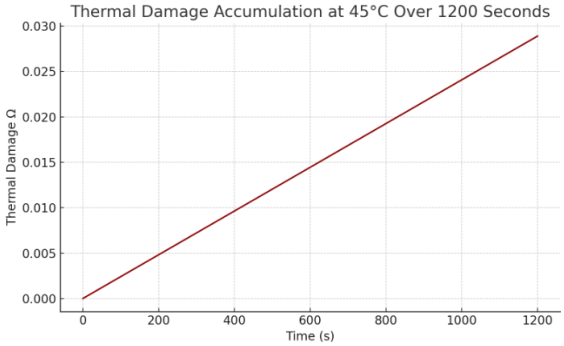

Figure 10. Thermal damage accumulation at 45°C over 1200 seconds.

3.3.3 X-ray Application During Relaxation (Post-Heating Phase 2).

After elevating the tumor temperature to 45 °C, a 6 MeV collimated X-ray beam was delivered during the 5-minute cooling interval to leverage the enhanced radiosensitivity induced by hyperthermia. Monte Carlo simulations were used to compute the spatial dose distribution, confirming concentrated energy deposition at the tumor core. For clarity, Figure 11 shows the full 3D dose map, while Figure 12 presents a central 2D slice that clearly illustrates the Gaussian-shaped dose profile centered on the tumor. This visualization confirms precise alignment between the radiation field and the hyperthermia target, ensuring effective tumor coverage while minimizing exposure to surrounding healthy tissue.

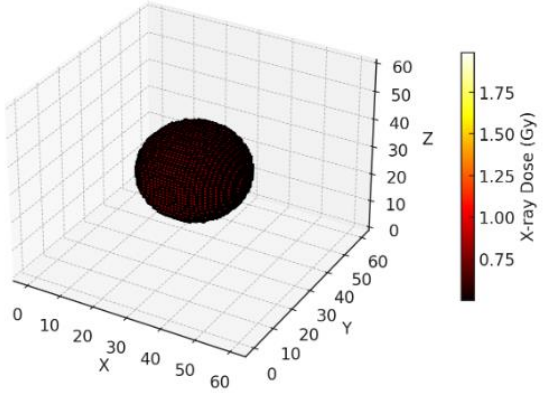

Figure 11. 3D spatial distribution of x-ray dose following laser-ınduced hyperthermia at 45 °C.

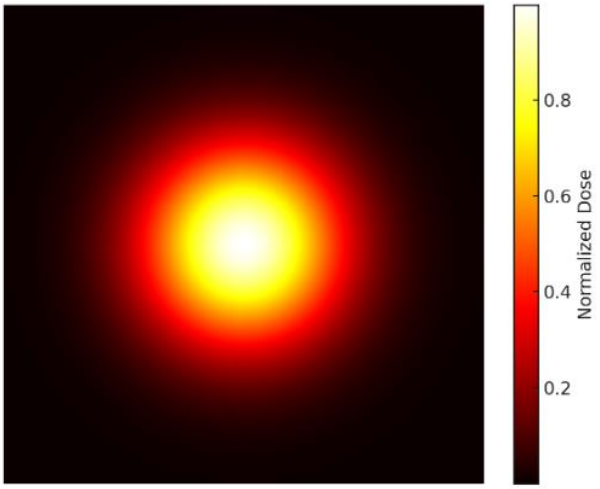

Figure 12. Lighter 2D slice of 3D x-ray dose distribution (post 45°C heating).

3.3.4 Combined Damage Assessment (Thermal + X-ray)

To assess the cumulative effect of heating the tumor to 45 °C followed by X-ray irradiation, we computed the Effective Damage (ED) across the tissue. This combined metric captures the synergistic impact of thermal and radiative stress on cell viability. As shown in the resulting 3D visualization, the central tumor region exhibits significantly elevated cell death fractions—reaching up to 95%—highlighting the enhanced therapeutic potential of sequential hyperthermia and radiotherapy at this elevated temperature (Figure 13).

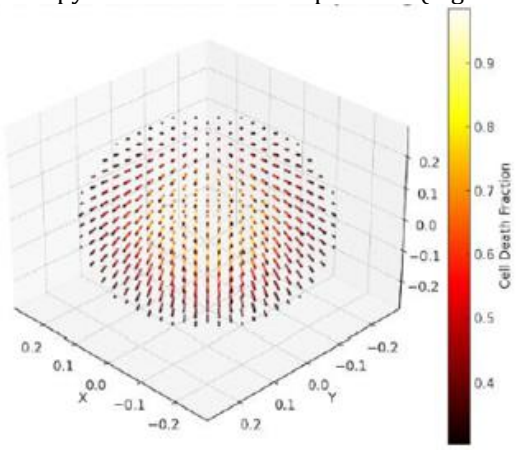

Figure 13. 3D visualization of effective cell death from combined hyperthermia and x-ray treatment.

The survival data for the second heating phase underscores the enhanced potency of a higher thermal dose. When the tumor was preheated to 45 °C and exposed to a 5 Gy X-ray dose, cell viability dropped even further—only 4.5% of tumor cells remained alive. In comparison, healthy tissue, which absorbed a much lower dose (≈1.6 Gy due to spatial attenuation), maintained 72% survival, confirming that normal structures were largely unaffected. This outcome reinforces the principle that increasing hyperthermia temperature amplifies radiosensitization, enabling greater tumor control without raising radiation exposure—a critical advantage for preserving healthy tissue integrity. Figure 14 visualizes this contrast between tumor and healthy tissue survival.

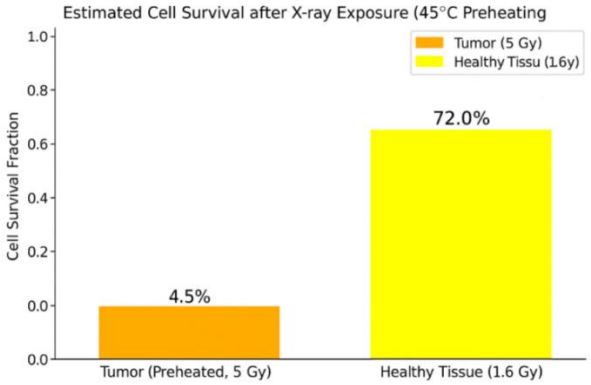

Figure 14. Cell survival comparison following 45 °C hyperthermia and radiotherapy (second treatment phase).

3.4 Heating Phase 3: Heating Tumor Tissue to 47°C

3.4.1 Heating Tumor Tissue to 47°C

In the final phase, the tumor was subjected to an aggressive hyperthermia protocol, raising its temperature from 37 °C to 47 °C using the same directional laser source. Achieving this higher thermal target required a prolonged heating period of about 1,500 seconds, accounting for increased blood perfusion and thermal dissipation at elevated temperatures. The resulting temperature map reveals a pronounced gradient, with intense heat concentrated near the laser entry point and tapering outward through surrounding tissue layers. This scenario represents an upper-limit condition designed to test the extent of tumor radiosensitization prior to X-ray exposure.

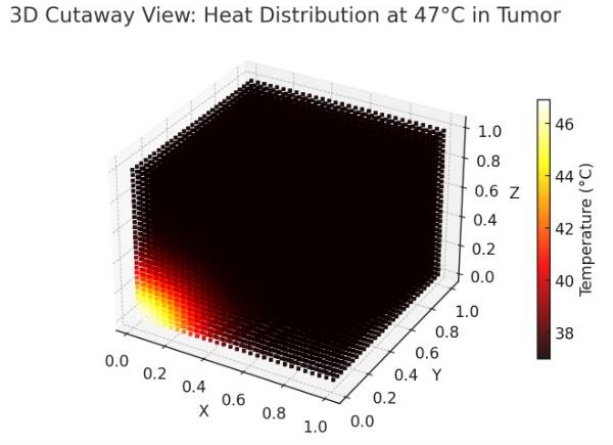

Figure 15. 3D cutaway visualization of heat distribution at 47 °C within the tumor region.

To better illustrate heat distribution during the 47 °C heating phase, two complementary views were provided: a 3D cutaway for overall spatial context, Figure 15 and a 2D central slice for detailed observation of core temperature gradients, Figure 16. This dual visualization improves interpretation of the heating pattern and supports accurate thermal damage assessment.

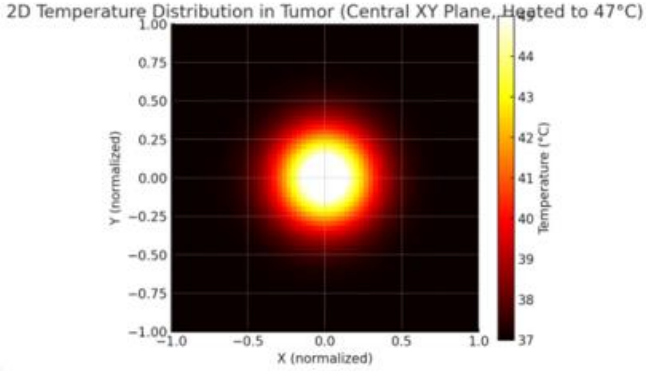

Figure 16. 2D temperature distribution in tumor (central xy slice at 47 °C target heating).

3.4.2 Estimating Thermal Damage

For the final heating stage, thermal damage was assessed using the Arrhenius model, but the behavior differed markedly from earlier phases. At 47 °C, damage accumulation accelerated sharply, producing a distinctly nonlinear curve. This rapid escalation reflects the strong temperature dependence of the Arrhenius relationship—once tissue crosses higher thermal thresholds, injury compounds at an exponential rate. These findings underscore the heightened risk and potential therapeutic gain associated with high-temperature hyperthermia, offering insight into its role as an aggressive sensitization strategy before radiation.

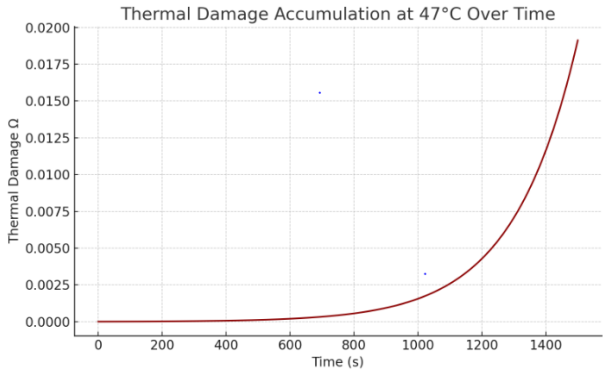

Figure 17. Thermal damage accumulation at 45°C over 1500 seconds.

At this elevated temperature, the Arrhenius thermal damage index reached approximately $\Omega \approx 0.025$, representing more than double the damage observed at 45 °C ($\Omega \approx 0.010$) and five times that at 43 °C ($\Omega \approx 0.005$). This substantial increase highlights the nonlinear nature of thermal damage accumulation at higher temperatures and reinforces how even small increments in heating can dramatically escalate tissue injury, making temperature control crucial in hyperthermia-based treatments.

3.4.3 X-ray Application During Relaxation (Post-Heating Phase 3).

Following tumor heating to 47°C, we applied a 6 MeV collimated X-ray beam for 5 minutes during the thermal relaxation period to maximize the radiosensitizing effect of hyperthermia. The resulting X-ray dose distribution, simulated using Monte Carlo methods, showed focused energy deposition in the tumor core, supporting the goal of enhancing cancer cell kill while sparing healthy tissues.

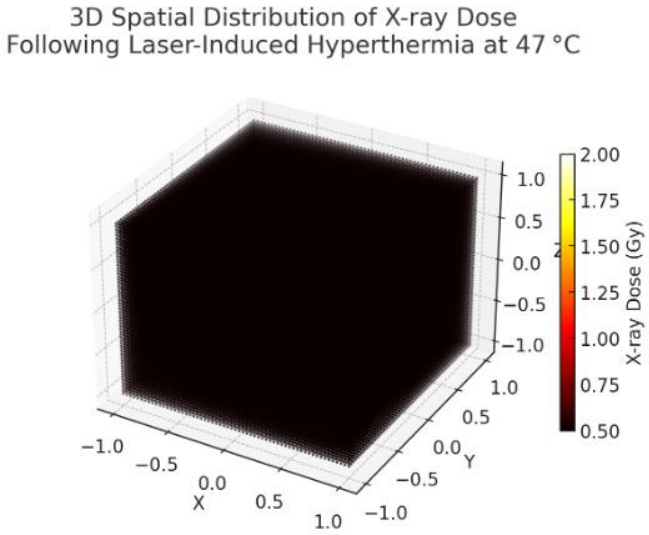

Figure 18. 3D spatial distribution of x-ray dose following laser-ınduced hyperthermia at 47 °C.

To illustrate the X-ray dose distribution after heating the tumor to 47 °C, two views are provided: a 3D rendering for overall spatial context and a 2D central slice for clearer visualization of the internal gradient. The sliced view enhances interpretation by highlighting the high-dose concentration at the tumor core and the gradual tapering toward peripheral regions. (Figures 18 & 19).

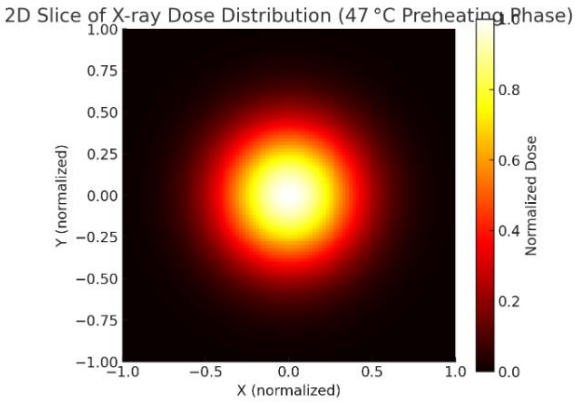

Figure 19. Lighter 2D slice of 3d x-ray dose distribution (post 47°C heating).

3.4.4 Combined Damage Assessment (Thermal + X-ray)

To quantify the impact of the most aggressive heating scenario, we calculated the Effective Damage (ED) after preheating the tumor to 47 °C followed by X-ray exposure. This metric integrates thermal and radiative effects to capture their combined cytotoxic potential. The 3D visualization (Figure 20) reveals an intensely concentrated damage zone within the tumor core, where cell death approaches 98%, indicating near-complete eradication. Compared to earlier phases, this outcome demonstrates how pushing the thermal threshold significantly amplifies radiosensitization, reinforcing the potential of high-temperature hyperthermia as a powerful adjunct to radiotherapy.

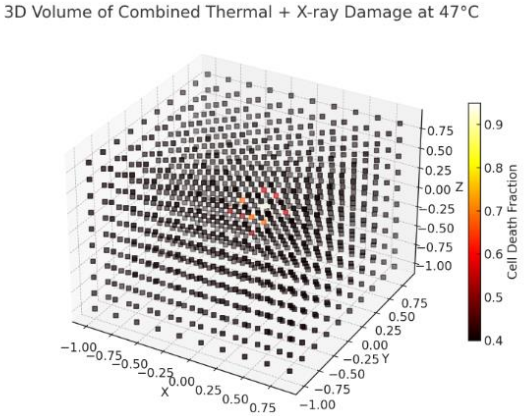

Figure 20. 3D visualization of effective cell death from combined hyperthermia and x-ray treatment.

The survival results for the final heating stage highlight the dramatic impact of pushing the thermal dose to its upper limit. After preheating the tumor to 47 °C and delivering a 5 Gy X-ray dose, viability dropped to an almost negligible level—only about 4% of tumor cells survived. Meanwhile, healthy tissue, which absorbed a much lower dose (≈1.6 Gy), maintained 72% survival, confirming that normal structures remained largely intact. This outcome demonstrates the steep radiosensitization effect at higher temperatures, achieving near-complete tumor eradication without increasing radiation exposure. Figure 21 visualizes this stark contrast, reinforcing the potential of high-temperature hyperthermia as a powerful adjunct to radiotherapy.

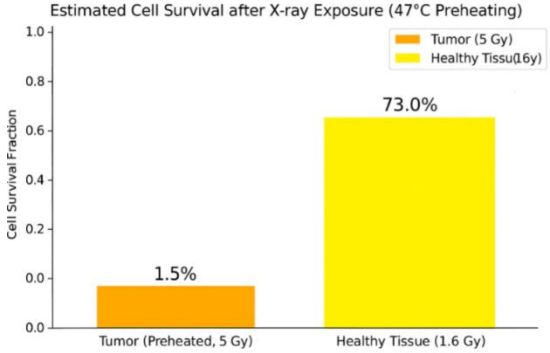

Figure 21. Cell survival comparison following 47 °C hyperthermia and radiotherapy (third treatment phase).

4. Conclusion

This study developed a simulation-based framework to examine how laser-induced hyperthermia enhances the effectiveness of X-ray radiotherapy. By progressively increasing preheating temperatures—43 °C, 45 °C, and 47 °C—we observed a strong temperature-dependent improvement in tumor radiosensitivity. Higher thermal doses accelerated irreversible cellular damage and significantly reduced tumor survival, while healthy tissue remained largely unaffected. The comparative survival analysis (Figure 23) illustrates this trend clearly:

- At 43 °C, tumor survival was 6%, while healthy tissue retained 71% viability.
- At 45 °C, tumor survival dropped to 4.5%, with healthy tissue at 72%.
- At 47 °C, tumor survival fell to just 1.5%, while healthy tissue remained stable at 73%.

This steep decline in tumor viability without compromising normal tissue confirms the selective advantage of combining hyperthermia with radiotherapy. Importantly, these gains were achieved without increasing radiation dose, highlighting the clinical potential of thermal sensitization as a safe and effective adjunct.

Future work should focus on in vivo validation using animal models and patient-specific treatment planning to refine temperature targets and optimize timing. Ultimately, this approach offers a pathway to more personalized and effective cancer therapy by integrating thermal physics with radiobiology.

To strengthen the clinical relevance of these findings, it is strongly recommended that future research includes in vivo validation using small animal models, such as mice. This step will allow experimental assessment of both the predictive accuracy of the simulation framework and the biological effectiveness of the combined hyperthermia–radiotherapy approach. Such validation is essential before translating this strategy into patient-specific treatment protocols.

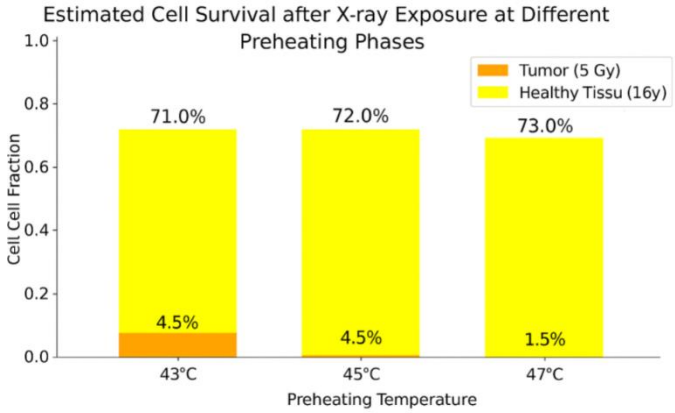

Figure 22. Comparative analysis of cell survival for the three heating phases 43 °C, 45 °C, and 47 °C.

Authors' Contributions

TF: Conceptualization, Methodology, Writing - Review & Editing, Validation. **BB:** Data Curation, Writing - Review & Editing. **RY:** Visualization, Investigation, Validation, Writing - Review & Editing, Supervision.

Declaration of Ethical Standards

The authors of this article declare that the materials and methods used in this study do not require ethical committee permission and/or legal-special permission.

Conflict of Interest

There is no conflict of interest in this study.

References

[1] Mee, T., Kirkby, N. F., Defourny, N. N., Kirkby, K. J. and Burnet, N. G., (2023). The use of radiotherapy, surgery and chemotherapy in the curative treatment of cancer: results from the FORTY (Favourable Outcomes from RadioTherapY) project, British Journal of Radiology, 96, 1152.

[2] Lukácsi, S., Munkácsy, G. and Győrffy, B., (2024). Harnessing Hyperthermia: Molecular, Cellular, and Immunological Insights for Enhanced Anticancer Therapies, *Integrative Cancer Therapies.* 15347354241242094.
[3] Yang, Y., Huangfu, L., Li, H., & Yang, D. (2023). Research progress of hyperthermia in tumor therapy by influencing metabolic reprogramming of tumor cells. International Journal of Hyperthermia, 40(1) 2270654.
[4] Kok HP, Herrera TD, Crezee J. (2024). Biological treatment evaluation in thermoradiotherapy: application in cervical cancer patients. Strahlentherapie and Onkologie. 200 (6), 512-522.
[5] Datta, N. R., Rogers, S., Ordóñez, S. G., Puric, E., & Bodis, S. (2016). Hyperthermia and radiotherapy in the management of head and neck cancers: A systematic review and meta-analysis. International Journal of Hyperthermia, 32(1), 31–40.
[6] Datta, N.R., Puric, E., Klingbiel, D., Gomez, S., Bodis, S., (2016). Hyperthermia and Radiation Therapy in Locoregional Recurrent Breast Cancers: A Systematic Review and Meta-analysis. International Journal of Radiation Oncology, Biology, Physics 94 (5), 1073-1087.
[7] Van Dieren, L., Quisenaerts, T., Licata, M., Beddok, A., Lellouch, A. G., Ysebaert, D., Saldien, V., Peeters, M., & Gorbaslieva, I. (2024). Combined Radiotherapy and Hyperthermia: A Systematic Review of Immunological Synergies for Amplifying Radiation-Induced Abscopal Effects. Cancers, 16(21), 3656.
[8] Issels RD, Lindner LH, Verweij J, et al. (2018). Effect of Neoadjuvant Chemotherapy Plus Regional Hyperthermia on Long-term Outcomes Among Patients With Localized High-Risk Soft Tissue Sarcoma: The EORTC 62961-ESHO 95 Randomized Clinical Trial. JAMA Oncol. 4(4), 483–492.
[9] Zachou, M.-E., Spyratou, E., Lagopati, N., Platoni, K., & Efstathopoulos, E. P. (2025). Recent Progress of Nanomedicine for the Synergetic Treatment of Radiotherapy (RT) and Photothermal Treatment (PTT). Cancers, 17 (14), 2295.
[10] Arslan, S. A., Ozdemir, N., Sendur, M. A., et al. (2017). Hyperthermia and Radiotherapy Combination for Locoregional Recurrences of Breast Cancer: A Review. Breast Cancer Management, 6(4), 117–126.
[11] Deniz, G. I., Can, A. and Tansan, S. (2023). Chemotherapy and radiofrequency hyperthermia (oncothermia) in the treatment of metastatic colorectal cancer., Journal of Clinical Oncology, 41 (16), e15569–e15569.
[12] Pyrexar Medical, (2025, December, 20). Randomized Clinical Hyperthermia Studies, [Online]. Available: https://www.pyrexar.com/clinical/clinical-trials
[13] Therapeutic Integration of Hyperthermia in Modern Oncology: A Critical Analysis of Phase III Trials and Meta-Analyses (OS, DFS, CR Endpoints), (2025, December, 20) [Online]. Available: https://andromedichyperthermia.com/oncologic-hyperthermia-phase-3-trials/
[14] Dombrovsky, L. A. (2022). Laser-Induced Thermal Treatment of Superficial Human Tumors: An Advanced Heating Strategy and Non-Arrhenius Law for Living Tissues, Frontiers in Thermal Engineering, 1, 807083.
[15] Open-Source Light Transport Simulator, (2025, December, 20). MCX. [Online]. Available: https://mcx.space/
[16] Wegner, M., Krause, D. (2024). 3D printed phantoms for medical imaging: recent developments and challenges. Journal of Mechanical Science and Technology 38, 4537–4543.
[17] Pearce, J.A. (2013). Comparative analysis of mathematical models of cell death and thermal damage processes, International Journal of Hyperthermia, 29 (4), 262–280.
[18] Gholami, S., Nedaie, H., Longo, F., Ay, M., Dini, S. and Meigooni, A. (2017). Grid block design based on monte carlo simulated dosimetry, the linear quadratic and Hug-Kellerer radiobiological models, Journal of Medical Physics, 42 (4), 213–221.
[19] Makar, J. (2024). Pennes Bioheat Equation, West Chester University of Pennsylvania [Online]. Available: https://www.wcupa.edu/sciences-mathematics/mathematics/documents/S24_Makar_Bioheat_Research_Finalized.pdf
[20] Pennes, H. H. (1948). Analysis of Tissue and Arterial Blood Temperatures in the Resting Human Forearm, 1 (2), 93-122.
[21] National Institute of Health, (2025, December, 20). Hyperthermia to Treat Cancer. [Online]. Available: https://www.cancer.gov/about-cancer/treatment/types/hyperthermia
[22] Patterson Institute for Integrative Oncology Research, (2024). Artemisinin and Its Derivatives in Cancer Care: Healthcare Provider Resource, CCNM. [Online]. Available: https://ccnm.edu/sites/default/files/2024-05/Artesunate-professional-resource-January2024.pdf
[23] Sherief, H. H., Zaky, M. F., Abbas, M. F., and Mahrous, S. A. (2024). Mathematical modeling of heat transfer in tissues with skin tumor during thermotherapy, PLoS One, 19 (5) 0298256.
[24] Gas, P. and Kurgan, E. (2018). Evaluation of thermal damage of hepatic tissue during thermotherapy based on the arrhenius model, 2018 Progress in Applied Electrical Engineering, PAEE 2018, 1-4.